Molecular Vision 2018; 24:443-458 <http://www.molvis.org/molvis/v24/443>
Received 29 November 2017 | Accepted 17 July 2018 | Published 19 July 2018

Expression patterns of *dscam* and *sdk* gene paralogs in developing zebrafish retina

Carlos A. Galicia,[1] Joshua M. Sukeena,[1] Deborah L. Stenkamp,[1] Peter G. Fuerst[1,2]

[1]University of Idaho, Department of Biological Sciences, Moscow, ID; [2]University of Washington School of Medicine, WWAMI Medical Education Program, Moscow, ID

Purpose: The differential adhesion hypothesis states that a cell adhesion code provides cues that direct the specificity of nervous system development. The Down syndrome cell adhesion molecule (DSCAM) and sidekick (SDK) proteins belong to the immunoglobulin superfamily of cell adhesion molecules (CAMs) and provide both attractive and repulsive cues that help to organize the nervous system during development, according to the differential adhesion hypothesis. The zebrafish genome is enriched in *dscam* and *sdk* genes, making the zebrafish an excellent model system to further test this hypothesis. The goal of this study is to describe the phylogenetic relationships of the paralogous CAM genes and their spatial expression and co-expression patterns in the embryonic zebrafish retina.

Methods: Exon–intron structures, karyotypic locations, genomic context, and amino acid sequences of the zebrafish CAM genes (*dscama*, *dscamb*, *dscaml1*, *sdk1a*, *sdk1b*, *sdk2a*, and *sdk2b*) were obtained from the Ensembl genome database. The Prosite and SMART programs were used to determine the number and identity of protein domains for each CAM gene. The randomized axelerated maximum likelihood (RaxML) program was used to perform a phylogenetic analysis of the zebrafish CAM genes and orthologs in other vertebrates. A synteny analysis of regions surrounding zebrafish CAM paralogs was performed. Digoxigenin (dig)-labeled cRNA probes for each CAM gene were generated to perform in situ hybridization of retinal cryosections from zebrafish embryos and larvae. Dual in situ hybridization of retinal cryosections from zebrafish larvae was performed with dig- and fluorescein-labeled cRNA probes.

Results: We found the studied zebrafish CAM genes encode similar protein domain structures as their corresponding orthologs in mammals and possess similar intron–exon organizations. CAM paralogs were located on different chromosomes. Phylogenetic and synteny analyses provided support for zebrafish *dscam* and *sdk2* paralogs having originated during the teleost genome duplication. We found that *dscama* and *dscamb* are co-expressed in the ganglion cell layer (GCL) and the basal portion of the inner nuclear layer (INL), with weak expression in the photoreceptor-containing outer nuclear layer (ONL). Of the *dscam* genes, only *dscamb* was strongly expressed in ONL. *Sdk1a* and *sdk1b* were co-expressed in the GCL and the basal portion of the INL. *Sdk2a* and *sdk2b* also showed co-expression in the GCL and basal portion of the INL. All *Sdk* genes were expressed in the ciliary marginal zone (CMZ). Dual in situ hybridizations revealed alternating patterns of co-expression and exclusive expression for the *dscam* and *sdk1* paralogs in cells of the GCL and the INL. The same alternating pattern was observed between *dscam* and *sdk2* paralogs and between *sdk1* and *sdk2* paralogs. The expression of *dscaml1* was observed in the INL and the GCL, with some cells in the basal portion of the INL showing co-expression of *dscaml1* and *dscama*.

Conclusions: These findings suggest that zebrafish *dscam* and *sdk2* paralogs were likely the result of the teleost whole genome duplication and that all CAM duplicates show some differential expression patterns. We also demonstrate that the comparative expression patterns of CAM genes in the zebrafish are distinct from the exclusive expression patterns observed in chick retina, in which retinal ganglion cells express one of the four chick *Dscam* or *Sdk* genes only. The patterns in zebrafish are more similar to those of mice, in which co-expression of *Dscam* and *Sdk* genes is observed. These findings provide the groundwork for future functional analysis of the roles of the CAM paralogs in zebrafish.

The differential adhesion hypothesis proposes that the organization of an organism's body plan is mediated by the expression of cell adhesion molecules that results in the aggregation of cells into different tissues and organs [1]. Experimental evidence for the differential adhesion hypothesis in the nervous system, where it is invoked to explain complex connectivity patterns, is robust. For example, neuroligins and neurexins, interacting families of cell adhesion molecules, have been experimentally demonstrated to provide specificity during neural development by partnering pre- and postsynaptic cells [2]. Other cell adhesion molecules, including cadherins, contactins, Dscams, semaphorins, and plexins, have also been implicated in patterning the nervous system by promoting adhesion or avoidance [3-8].

Many studies on the role of differential adhesion in neural development have been conducted vis-à-vis the retina. Unlike other neural tissues, retinal neurons locate and form synapses with the appropriate partners in the absence

Correspondence to: Deborah L. Stenkamp, Department of Biological Sciences University of Idaho, Moscow, Idaho 83844; Phone: (208) 885-8963; FAX: (208) 885-7905; email: dstenkam@uidaho.edu

of synaptic input [9], which then play a more local role in sculpting precise synaptic structures in the retina [10,11]. The retina is organized into three layers—the outer nuclear layer (ONL), which contains rod and cone photoreceptors; the inner nuclear layer (INL), which contains bipolar, amacrine, and horizontal cells; and the retinal ganglion cell layer (GCL), which contains ganglion and displaced amacrine cells [12]. Retinal synapses are localized to two synaptic layers located in between the cellular layers, the outer plexiform layer (OPL) and the inner plexiform layer (IPL). The abundance of tools to label and manipulate retinal neurons and the importance of the tissue in our species dominant sense, vision has made the retina a valuable model to study the mechanisms of neural connectivity.

The zebrafish retina is an exceptionally good model to study the mechanisms by which differential adhesion sculpts neural architecture. This is in part because zebrafish, as members of the teleost lineage of fishes, underwent a whole genome duplication (WGD) event approximately 400 million years ago (mya) [13]. As a result, many genes represented by a single copy in tetrapods have two homologs in zebrafish. Following duplication, a gene may be neofunctionalized (a new function emerges), subfunctionalized (each of the gene products adopts some of the functions of the original gene, possibly tissue- or developmental stage-dependent), or, most commonly, pseudogenized (loss of expression and/or function of one gene copy) [14]. Potential subfunctionalized and neofunctionalized gene paralogs in the zebrafish genome present the opportunity to dissect the function(s) of genes that play multiple critical roles in neural development. For example, a loss of function of only one paralog in zebrafish may generate a phenotype that is simpler to interpret than a corresponding mouse or human phenotype [15]. For cell adhesion molecules, the study of subfunctionalized paralogs would further our understanding of the differential adhesion hypothesis.

As a first step, we have characterized the expression of Down Syndrome cell adhesion molecule (*dscam*), and sidekick (*sdk*) paralogs in the zebrafish retina. DSCAM and SDK proteins in other model organisms have been implicated in multiple developmental roles, including axon guidance, avoidance, and synaptic targeting [16-20]. The zebrafish genome has three *dscam* genes (*dscama*, *dscamb*, and *dscaml1*) and four *sdk* genes (*sdk1a*, *sdk1b*, *sdk2a*, and *sdk2b*), while the chick and mouse genomes each contain only two *Dscam* genes (*Dscam* and *Dscaml*) and two *Sdk* genes (*Sdk1* and *Sdk2*). In this study, we examine the comparative predicted protein structure and phylogenetic relationships of the zebrafish *dscam* and *sdk* genes and determine their respective expression patterns in the developing zebrafish retina.

METHODS

Animals and tissue processing: Wild-type strains of zebrafish (*Danio rerio*) were maintained on a 14 h:10 h light:dark cycle in monitored, recirculating system water according to standard protocols, as previously described [21]. All procedures using animals were approved by the University of Idaho's Institutional Animal Care and Use Committee. Embryos were collected and maintained at 28.5 °C until collecting at 48, 72, and 96 h post fertilization (hpf). The time of spawn was considered as 0 hpf. Embryos/larvae were fixed in a solution of 4% paraformaldehyde in 5% buffered (pH 7.4) sucrose. Following fixation, embryos/larvae were transferred in sequential steps of increasing the percentage of sucrose solution in phosphate buffer (PB) to 20% sucrose for overnight cryoprotection at 4 °C. Tissues were embedded in a mixture consisting of a 1:2 ratio of 20% sucrose in PB and optimal cutting temperature (OCT) embedding medium (Sakura Finetek USA, Torrance, CA). Tissues were frozen and sectioned into 5 µm samples using a Microm HM 550 cryostat or a Leica CM3050 cryostat.

Sequence analysis: Amino acid sequences of proteins encoded by the zebrafish (*dscama*, *dscamb*, *dscaml1 sdk1a*, *sdk1b*, *sdk2a*, and *sdk2b* genes) were obtained from the Ensembl genome database (ensembl.org release 90). The longest protein coding transcript was used in all analyses. The amino acid sequence of the genes was analyzed using the SMART [22] and Prosite [23] programs to determine the number and identity of protein domains (Figure 1A). The intron–exon structure and the position of genes in chromosomes were obtained from Ensembl (release 90; Figure 1B,C).

Phylogenetic analysis: Amino acid sequences for zebrafish Dscama, Dscamb, Dscaml1, Sdk1a, Sdk1b, Sdk2a, Sdk2b and their orthologs in medaka (*Oryzias latipes*), tilapia (*Oreochromis niloticus*), threespine stickleback (*Gasterosteus aculeatus*), cod (*Gadus morhua*), humans (*Homo sapiens*), mice (*Mus musculus*), chickens (*Gallus gallus*), and spotted gar (*Lepisosteus oculatos*) were obtained from Ensembl (release 90). Alignments for the amino acid sequences were generated with ClustalW [24] using a BLOSUM cost matrix. Gaps were removed from the alignments. Gene trees were generated with randomized axelerated maximum likelihood (RaxML) 8.2.11 [25] using an algorithm for rapid bootstrapping and search for the best score maximum likelihood tree under the model gamma blosum62.

Synteny analysis: Images of regions of the zebrafish genome with annotated genes near the locations of the *dscam* and *sdk*

genes were obtained from Ensembl (release 92). The identities of the annotated genes and their paralogs were confirmed through a BLAST alignment.

Probe preparation: Zebrafish larvae (96 hpf) were homogenized in 1.0 mL of TRIzol reagent (Invitrogen, Waltham, MA, USA), and RNA was extracted using a PureLink RNA Micro Kit (Invitrogen). The extracted RNA was used to generate cDNA with qScript cDNA SuperMix (Quanta Bioscience, Saskatoon, SK, Canada). The resulting cDNA library was subjected to PCR using gene-specific primers. The resulting PCR products were run and isolated on 0.75% agarose gel and purified using a GeneJet Gel Extraction Kit (Fermentas Life Technologies, Waltham, MA). The purified DNA was TA cloned into a T-easy vector (Promega, Madison, WI) and used to generate cRNA probes through in vitro transcription using DIG RNA labeling mix (Roche, Indianapolis, IN) and T7 or SP6 RNA polymerase (Roche). The primers and promoter sequences corresponding with each gene target are summarized in Table 1.

Histological processing and in situ hybridization: In situ hybridization was performed as previously described in [26-28]. Sections were vacuum dried for 24 h before storage at -20 °C. They were then hydrated using sequential ethanol treatments at concentrations of 100%, 95%, 70%, and 50%. Proteinase K was used to permeabilize the tissue, and this was followed by acetylation with triethanolamine (TEA) and acetic anhydride. Sections were then dehydrated with sequential ethanol treatments at concentrations of 50%, 75%, 95%, and 100% before air drying for 1 h. Tissues were hybridized with probes for *dscama*, *dscamb*, and *dscaml1* at 68 °C. Probes for *sdk1a*, *sdk1b, sdk2a*, and *sdk2b* were hybridized at 70 °C. These hybridization temperatures were selected according to Polypro software [29]. Following stringency washes of 1:1 formamide and 2xSSC performed at 65 °C,

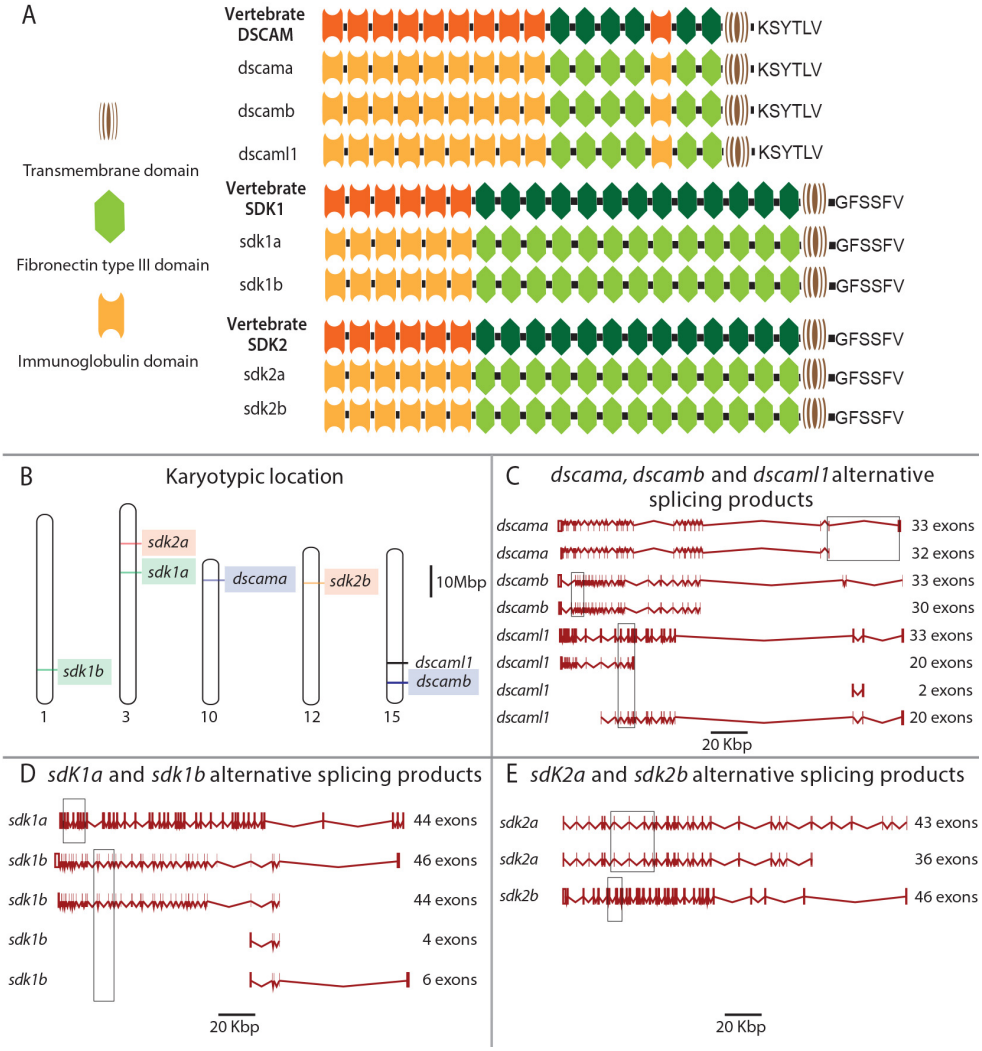

Figure 1. Comparison of the protein and gene structure of vertebrate *Dscam* and *Sdk* genes. **A**: The combination of domain structures for zebrafish Dscama, Dscamb, Dscaml1, Sdk1a, Sdk1b, Sdk2a, and Sdk2b proteins as predicted from the zebrafish genome. The corresponding structures for Dscam, Sdk1, and Sdk2 for other non-teleost vertebrates are also displayed. **B**: Positions of *dscam* and *sdk* genes in the zebrafish genome. Chromosome numbers are shown as 1, 3, 10, 12, and 15. Paralogs are highlighted with the same colors. Scale bar=10 Mbp. **C–E**: The predicted exon–intron structures for zebrafish *dscam* and *sdk* genes obtained from Ensembl (release 90). Rectangles indicate exon locations targeted by RNA antisense probes. Scale bars=20 Kbp. Abbreviations: Dscam=Down syndrome cell adhesion molecule; Sdk=sidekick; Kbp=Kilo base pairs; Mbp=Mega base pairs.

Table 1. Primer sequences used to amplify genes and generate corresponding probes and percentage similarity of the resulting probe.

Gene	Forward (5′–3′)	Reverse (5′–3′)	% similarity (to most similar CAM gene)
dscama	GCTCTGAGTCCAGCTGAGAAA	GGATCCCTGGGACGTTGTAG	83% (*dscamb*)
dscamb	CGTACACCTGACACCGTGAA	TTGTTTGCTTGTCGTTGCCG	79% (*dscama*)
dscaml1	GGGCTCATCCAGCTGACAAA	TCTCCCCATTCTCCATCGGG	66% (*dscama*)
sdk1a	CTCTTCCGACCGGAAACCAA	GCTGTTCCACAGCTCTTGT	69% (*sdk1b*)
sdk1b	CAGGTGCTCGCATTTACACG	GCCTGAGGACGCTCTTTTTG	72% (*sdk1a*)
sdk2a	CCCCTACAGTGTGAGGAACC	GGCGTACAGGGCTCATAGAC	77% (*sdk2b*)
sdk2b	GCTGGGCAGAACTCACATCT	TGAAGACAGTCGACACAGGC	77% (*sdk2a*)

tissue was treated with RNase A and then incubated overnight at room temperature in anti-digoxigenin-AP, Fab fragments or anti-fluorescein-AP, Fab fragments (Roche). NBT/BCIP solution and/or Fast Red were used to generate colored precipitates. Dual in situ hybridization was performed as previously described [30]. Upon completion of color development, slides were washed in alkaline phosphatase (AP) buffer and mounted with 80% glycerol. Images were collected using a Leica DMR microscope and a SPOT camera or a Leica DM2500 upright microscope with a Leica DFC700T camera using bright-field or differential interference contrast (DIC) optics. Each probe was examined using at least four slides containing tissue from at least three different embryos/larvae for each sampling time. Sense probes were prepared and did not generate a detectable signal.

RESULTS

Overview of the cell adhesion molecule genes and phylogenetic and synteny analyses: DSCAM and SDK proteins belong to the immunoglobulin superfamily (IgSF) of CAMs. The structure of these proteins includes a variable number of immunoglobulin-like domains, a variable number of fibronectin domains (type III), a single-pass transmembrane domain, and an intracellular domain with a C-terminus that binds to the PDZ domain of an interacting protein [31–34] (Figure 1A). Genome analysis reveals that zebrafish *dscama*, *dscamb*, *dscaml1*, *sdk1a*, *sdk1b*, *sdk2a*, and *sdk2b* each encode similar protein domain patterns, which corresponds to what has been shown previously in their respective orthologs in other vertebrates [35] (Figure 1A). The presence of introns in all CAM genes analyzed indicates that paralogous genes were not duplicated by retrotransposition events, as these events would result in intronless genes [36]. D*scaml1* and *dscamb* were found to be located on chromosome 15, *dscama* was found to be located on chromosome 10, *sdk1a* and *sdk2a* were found to be located on chromosome 3, *sdk1b* was found to be located on chromosome 1, and *sdk2b* was found to be located on chromosome 12 (Figure 1B). Data obtained from Ensembl (GRCz10) indicated that *dscama* is predicted to have 32–33 exons, *dscamb* is predicted to have 30–33 exons, and *dscaml1* is predicted to have four alternative splice products with a variable number of exons (Figure 1C). *Sdk1a* is predicted to have a single splice product of 44 exons, and *sdk1b* is predicted to have four alternative splice products with a variable number of exons (Figure 1D). *Sdk2a* and *sdk2b* are predicted to possess 43 and 36 or 46 exons, respectively (Figure 1E). Unlike *Drosophila Dscam1*, which has an estimated 38,000 splice variants, tetrapod *dscam* and *sdk* genes undergo only limited alternative splicing [16,37-39]. The limited number of alternative splice forms in zebrafish is consistent with the splicing patterns of tetrapod *dscam* and *sdk* genes (Figure 1C–E).

Individual phylogenetic trees were generated using amino acid sequences for Dscaml1 and each pair of Dscam, Sdk1 and Sdk2 paralogs using RaxML. The phylogenetic analysis for each set of genes included amino acid sequences corresponding to orthologs from the teleost fish—medaka (*Oryzias latipes*), tilapia (*Oreochromis niloticus*), threespine stickleback (*Gasterosteus aculeatus*), and cod (*Gadus morhua*). In addition, we included orthologs from humans (*Homo sapiens*), mice (*Mus musculus*), chickens (*Gallus gallus*), and spotted gar (*Lepisosteus oculatos*) that diverged from the teleost lineage before the teleost genome duplication (TGD) [40].

The resulting tree for Dscam showed Dscama and Dscamb orthologs from teleost fish grouped into two different branches. Spotted gar Dscam was placed as diverging before the duplication that gave rise to the two branches of Dscam paralogs in teleost fish (Figure 2A), consistent with these paralogs emerging with the TGD.

The DSCAML1 tree grouped teleost Dscaml1 duplicates into two branches (albeit with low confidence); however, zebrafish Dscaml1 was placed diverging before the branches of Dscaml1 paralogs in teleosts, and the spotted gar Dscaml1 was placed diverging before the zebrafish Dscaml1 and teleost Dscaml1 paralogs diverged (Figure 2B). The branch point for zebrafish Dscaml1 versus Dscaml1 of the other teleosts examined likely diverged before speciation events, leading to the cyprinid lineage (such as zebrafish). Cyprinids, or specifically zebrafish, may not have retained any duplicated *Dscaml1* gene(s) arising from the TGD.

In the SDK1 tree, zebrafish Sdk1a was grouped with spotted gar Sdk1, while zebrafish Sdk1b was grouped with the Sdk1 genes of other teleost fish (Figure 2C). The SDK1 tree suggests that the *sdk1a* paralog that was retained in zebrafish could have emerged before the TGD, followed by the loss of both resulting genes' paralogs. Alternatively, this could be a result of the differential divergence of the paralogous *sdk1* genes in the teleost lineages, which is a more parsimonious explanation. Interestingly, the non-cyprinid teleosts that were sampled did not show evidence of duplicated *sdk1* genes in their genomes.

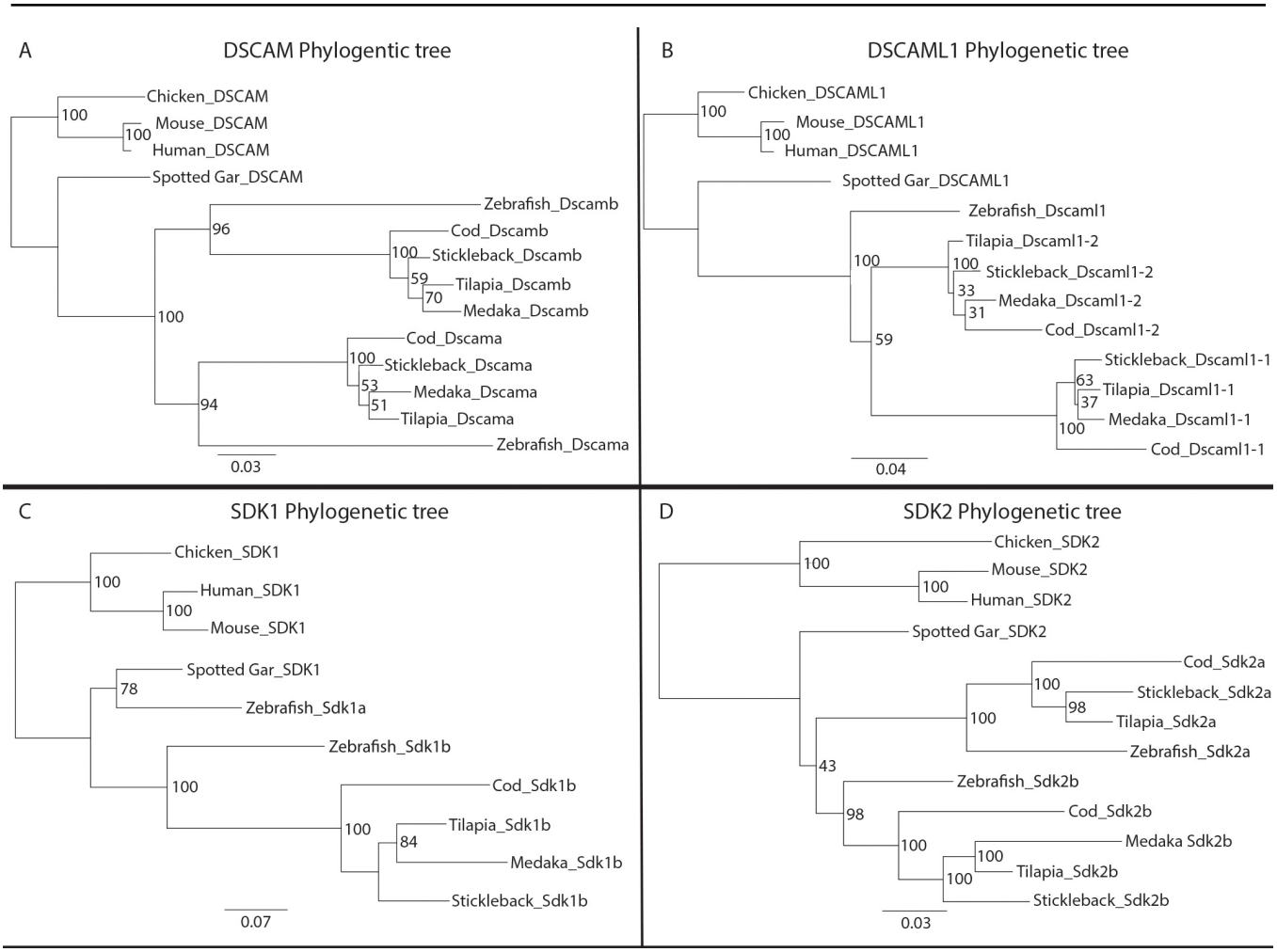

Figure 2. Phylogenetic analysis of Dscam and Sdk amino acid sequences of selected vertebrates. Individual maximum likelihood trees were generated by RaxML under the model gamma blosum62. Bootstrap support from maximum-likelihood analysis is shown at each node. Orthologs corresponding to DSCAM, DSCAML1, SDK1, and SDK2 from zebrafish (*Danio rerio*), medaka (*Oryzias latipes*), tilapia (*Oreochromis niloticus*), threespine stickleback (*Gasterosteus aculeatus*), cod (*Gadus morhua*), humans (*Homo sapiens*), mice (*Mus musculus*), chickens (*Gallus gallus*), and spotted gar (*Lepisosteus oculatos*) were used for the analysis. Roots are placed in non-fish vertebrates. Maximum likelihood trees for **A**) DSCAM **B**), DSCAML1 **C**), SDK1, and **D**) SDK2 orthologs are shown. The scale bar at the bottom indicates substitutions per site. The numbers at branch points indicate bootstrapping values. Abbreviations: Dscam=Down syndrome cell adhesion molecule; Sdk=sidekick.

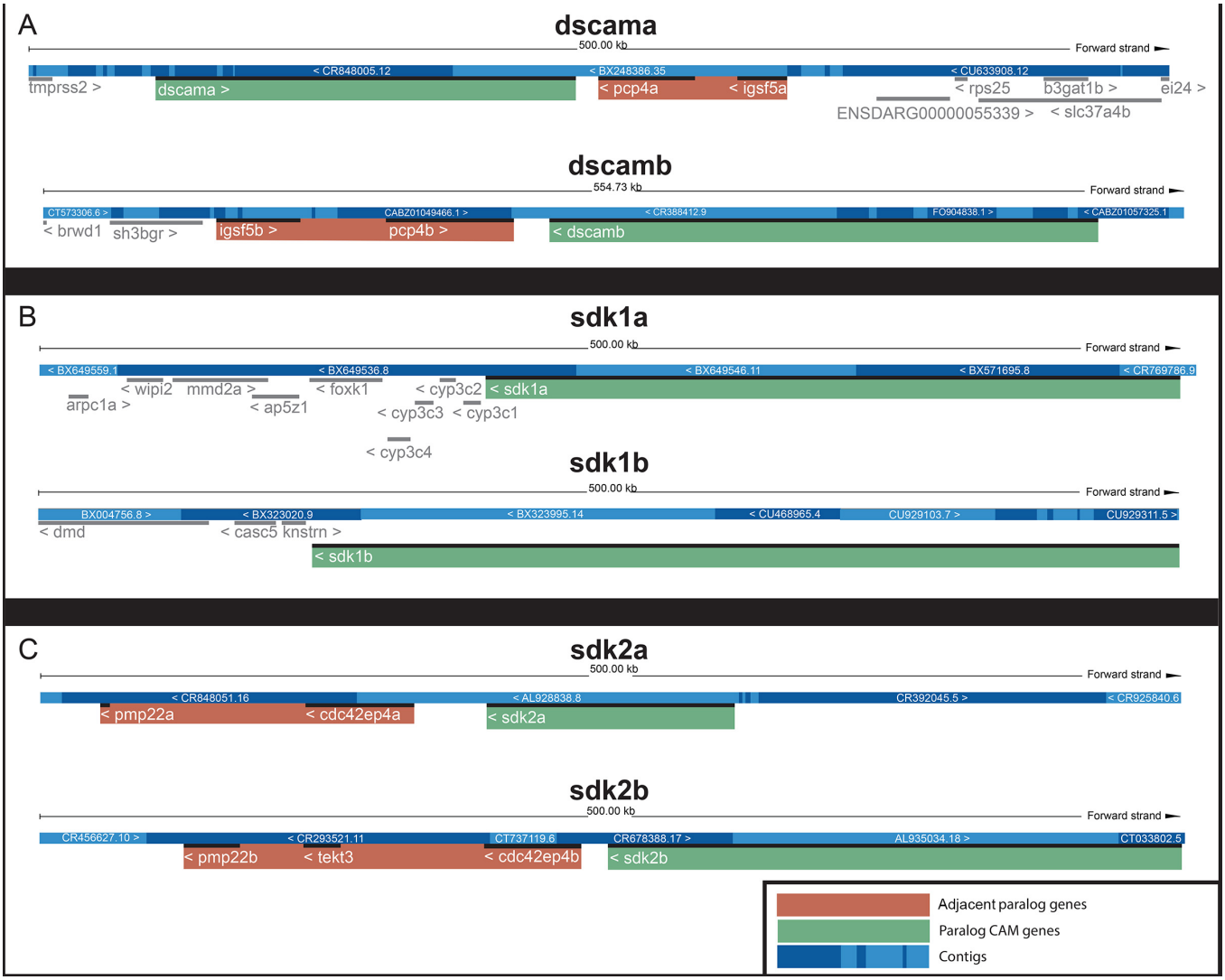

Figure 3. Synteny analysis of genomic locations of *dscam* and *sdk* paralogs. Locations of *dscam* and *sdk* genes shown from Ensembl release 92. Corresponding CAM paralogs are identified with green shading, and adjacent genes with corresponding paralogs are identified with orange shading. Adjacent contigs are identified with dark versus light blue shading.

In the SDK2 gene tree, Sdk2a and Sdk2b were grouped into two different branches, and spotted gar Sdk2 was placed diverging previous to the duplication of Sdk2 in teleosts (Figure 2C). These results are consistent with the Sdk2 paralogs emerging with the TGD.

The locations of paralogous genes on different chromosomes (Figure 1B) suggest that none of the paralogs were generated by local, tandem duplications. In addition, the presence of introns in all CAM genes analyzed (Figure 1C-E) indicates that paralogous genes were not duplicated by retrotransposition events, as these events would result in intronless genes [36]. Synteny analysis of *dscama/dscamb* and of *sdk2a/sdk2b* revealed the presence of multiple genes possessing corresponding paralogs around the duplicated portions of genome where the CAM paralogs are located, supporting duplications related to the TGD [41] (Figure 3). However, synteny analysis of *sdk1a/sdk1b* revealed nearby genes with no corresponding paralogs around the duplicated *sdk1*, leaving open the possibility of these paralogs having originated with events not related to the TGD (Figure 3).

Differential expression patterns of zebrafish dscam paralogs during retinogenesis: We used in situ hybridization to examine expression patterns for the *dscam* paralogs in the developing zebrafish retina. Transcript-specific probes were applied to cryosectioned retinal tissue obtained from zebrafish embryos/larvae sacrificed at 48, 72 and 96 h post

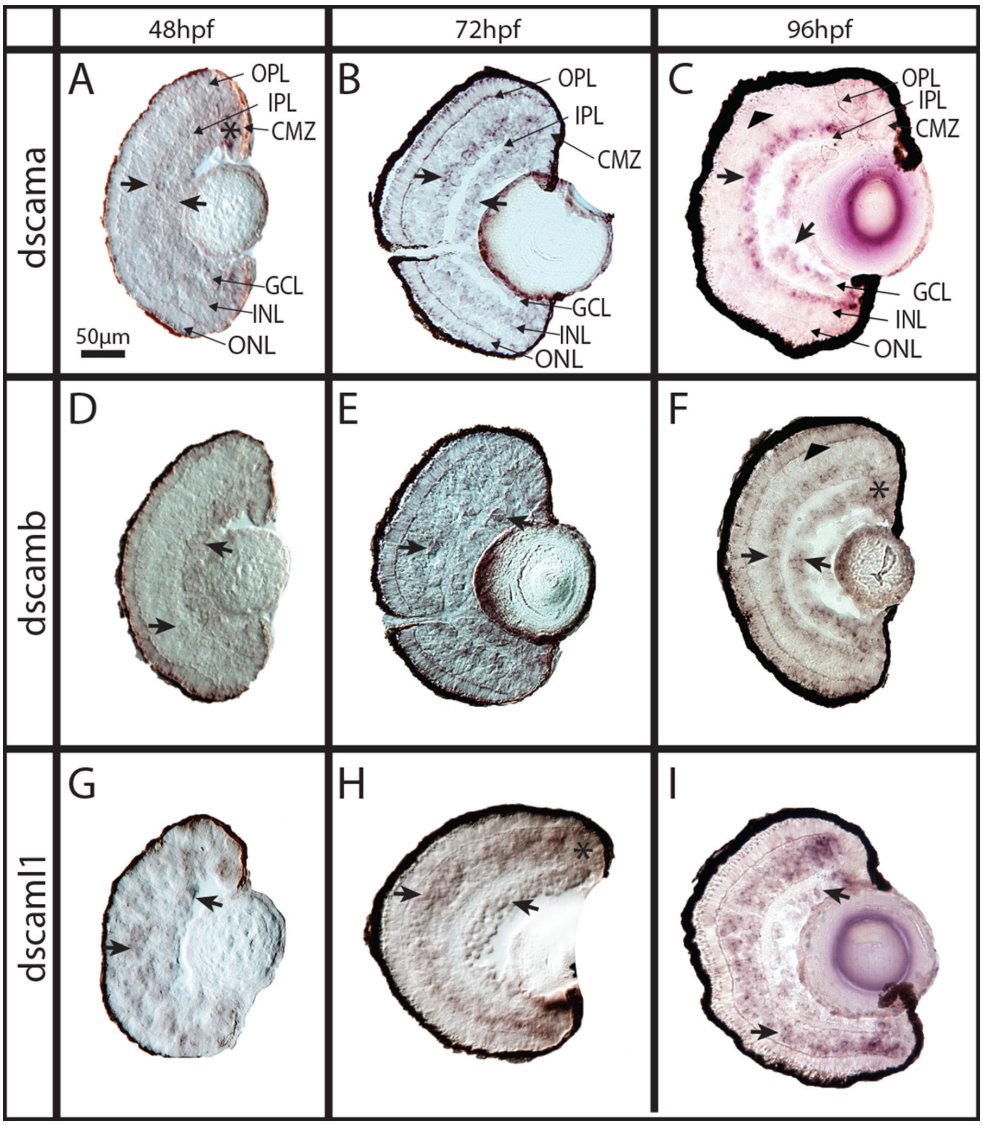

Figure 4. Expression of *dscam* genes in developing zebrafish retina. In situ hybridization using cryosections derived from 48, 72 and 96 hpf zebrafish retina is shown for **A–C**) *dscama*, **D–F**) *dscamb*, and **G–I**) *dscaml1*. Consistent labeling for all *dscam* genes was found in the INL and GCL (arrows in all panels); however, strong expression in the ONL was observed for *dscamb* (arrowheads in **F** versus **C**). **D–F**: Expression in the CMZ was also observed for **(A)** *dscama* at 48 hpf, (**F**) *dscamb* at 96 hpf, and (**H**; asterisk) *dscaml1* at 72 hpf. All images displayed are of sections processed with antisense probe. Abbreviations: hpf=hours post fertilization; Dscam=Down syndrome cell adhesion molecule; INL=inner nuclear layer; GCL=ganglion cell layer; IPL=inner plexiform layer; CMZ=ciliary marginal zone (asterisk). Scale bar in **A**=50 µm (applies to all).

fertilization (hpf). These times correspond to the emergence of the OPL (48 hpf), the onset of cone-mediated visual function (72 hpf), and continued retinal growth beyond the embryonic period (96 hpf) [42]. At 48, 72, and 96 hpf, *dscama* mRNA was expressed by a subset of cells located in the ganglion cell layer (GCL) and the basal portion of the INL, which corresponds to the location of amacrine cells, with weak expression in some cells of the ONL, where photoreceptors are located (Figure 4A–C). Likewise, *dscamb* mRNA was also detected in subsets of cells located in the GCL and basal portions of the INL. However, the *dscamb* signal was observed to be strongly expressed in the ONL (Figure 4D–F); this expression pattern was consistent for 48, 72 and 96 hpf samples. We previously found *dscamb* to be expressed in the ONL of adult zebrafish by in situ hybridization and to be enriched in the rod photoreceptors of adult zebrafish by RNA-Seq and qPCR of purified rods [43].

Expression of *dscaml1* mRNA was observed in patches of cells scattered throughout the INL and the GCL in 48, 72, and 96 hpf zebrafish retina (Figure 4G-I). The expression domains of *dscamb* mRNA and *dscaml1* mRNA appear to increase in size over developmental time, while the expression domain of *dscama* in the INL and the GCL appears to decrease in thickness over developmental time (Figure 4).

To ensure that the expression patterns observed were not products of artifacts produced by the microscopy method used, cryosections were also imaged under bright-field and DIC optics for direct comparison (Figure 5A,B,E,F,I,J). The bright-field images show patterns similar to those viewed under DIC optics. In addition, in situ hybridization

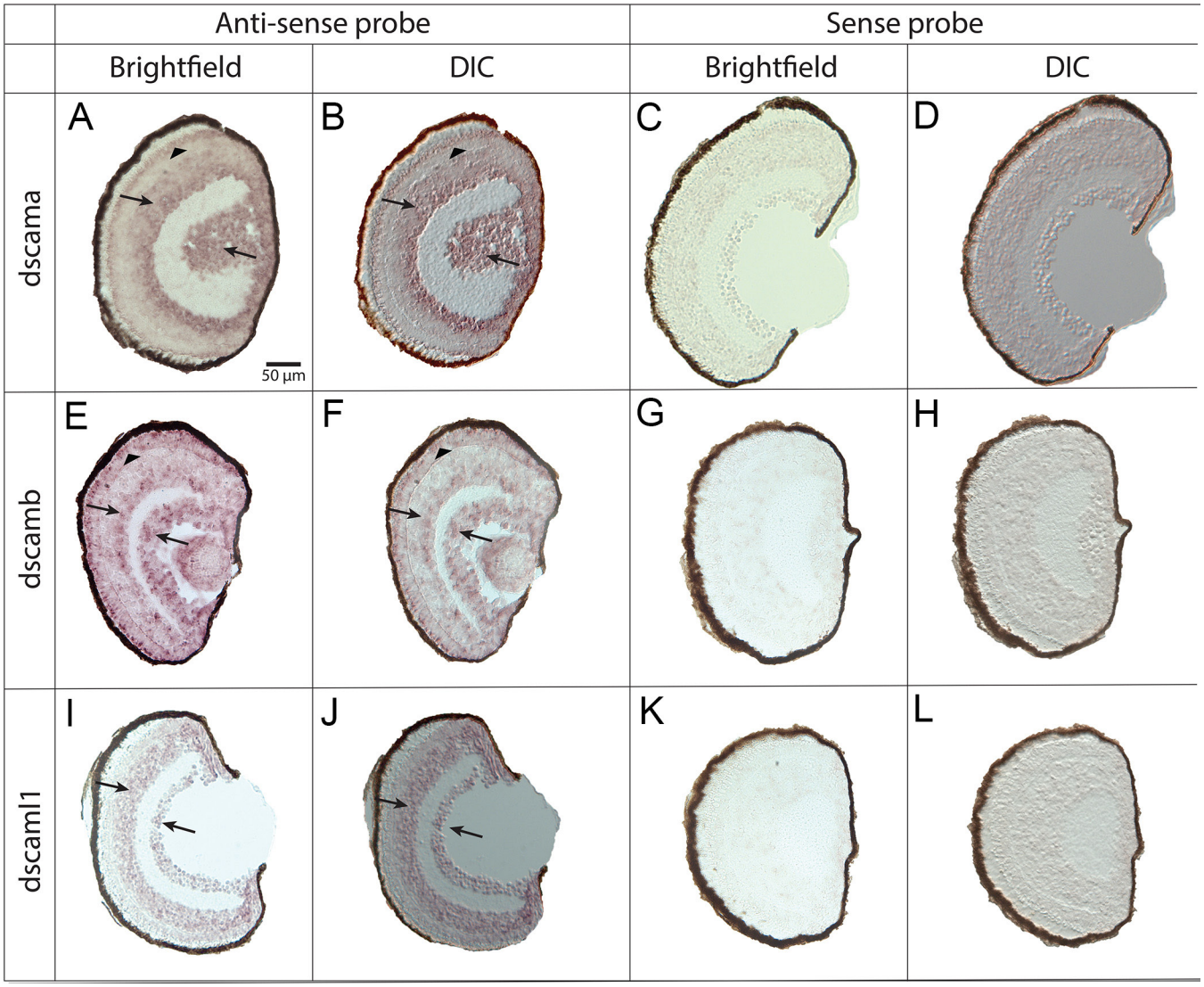

Figure 5. Bright-field and DIC imaging of antisense and sense in situ hybridization for *dscam* genes in cryosections. In situ hybridization using cryosections derived from 96 hpf zebrafish retina is shown for **A-D**) *dscama*, **E-H**) *dscamb*, and **C**) *dscaml1*. **A,B,E,F,I,J**) In situ hybridization performed with antisense probes is shown. Arrows point to labeling in the INL and ganglion cell layer (GCL); arrows point to labeling in the outer nuclear layer (ONL); and asterisks show labeling in the ciliary marginal zone (CMZ). **C,D,G,H,K,L**) In situ hybridization performed with sense probes is shown. **A,C,E,G,I,K**) Photographs of antisense and sense in situ hybridization taken under bright-field conditions are shown. **B,D,F,H,J,L**) Images of antisense and sense in situ hybridization collected using DIC microscopy are shown. Abbreviations: DIC=differential interference contrast; hpf=hours post fertilization; Dscam=Down syndrome cell adhesion molecule; Sdk=sidekick. Scale bar in A=50 µm (applies to all).

controls using sense probes were performed for each *dscam* gene and imaged under bright-field and DIC optics (Figure 5C,D,G,H,K,L). Sense probes did not produce a detectable reaction product.

Differential expression patterns of zebrafish sdk paralogs during retinogenesis: We used in situ hybridization to determine the mRNA expression patterns for the gene paralog pairs *sdk1a* and *sdk1b* and s*dk2a* and *sdk2b*. Antisense probes detected the expression of transcripts for all four genes in the basal region of the INL and in the GCL at 48, 72, and 96 hpf (Figure 6A–L). This predicts their expression by amacrine cells (AC) and retinal ganglion cells (RGCs). Sections from 96 hpf retina showed the expression of *sdk2a* and *sdk2b* in subsets of cells in the ONL (Figure 6I, L) and possibly weak expression of *sdk1a* and *sdk1b* in some cells of the ONL (Figure 6C–F). The patterns for *sdk2* transcripts are similar to the expression pattern seen for *dscamb* (Figure 6F). All four zebrafish *sdk* paralogs were detected in the ciliary marginal

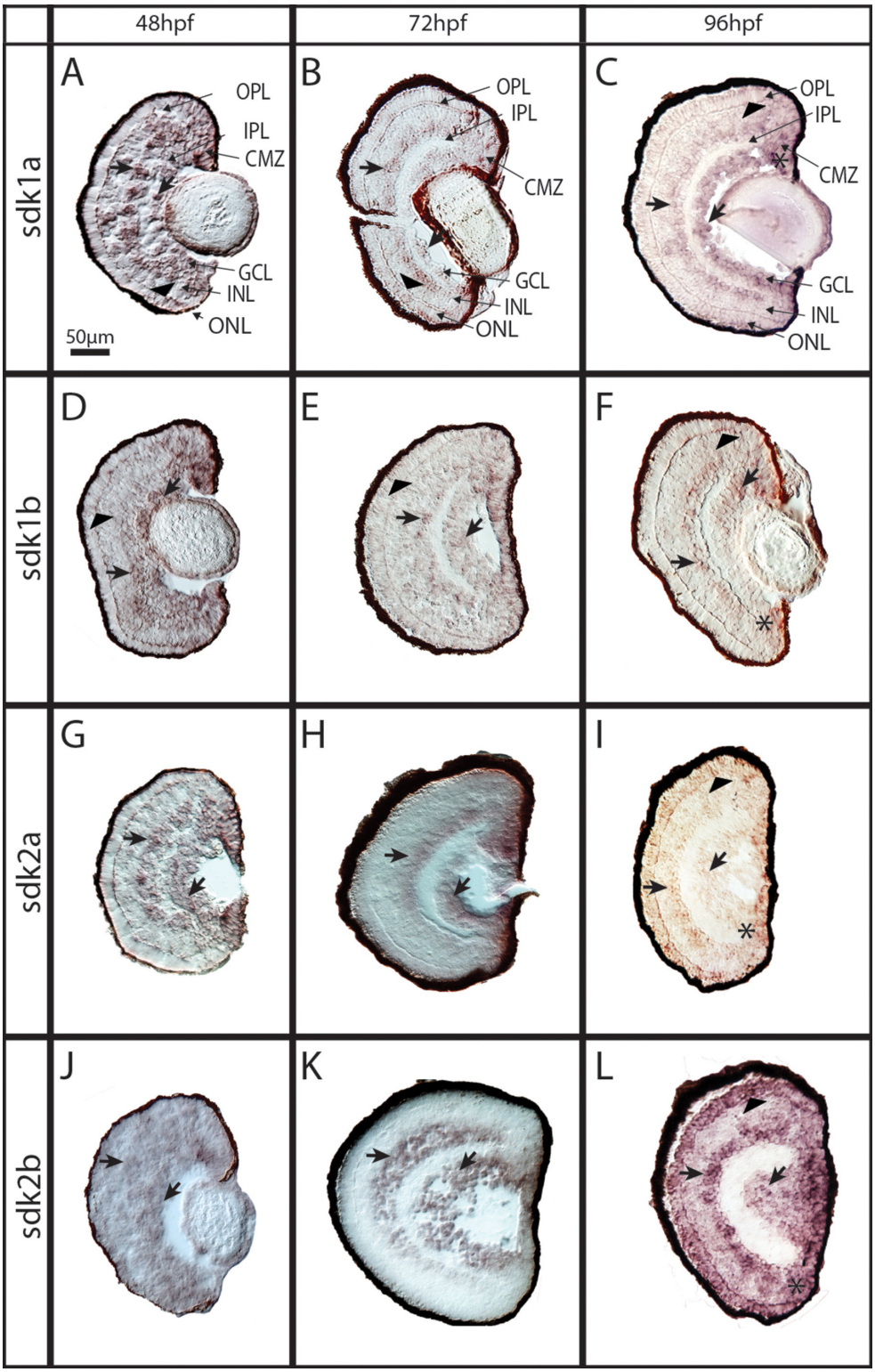

Figure 6. Expression of *sdk* genes in developing zebrafish retina. In situ hybridization using cryosections of 48, 72 and 96 hpf zebrafish retina is shown for **A–C**) *sdk1a*, **D–F**) *sdk1b*, **G–I**) *sdk2a*, and **J–L**) *sdk2b*. Consistent labeling for all *sdk* genes was found in the INL, the GCL (arrows in all panels), and the CMZ (asterisks); however, strong expression in the ONL was observed only for (**I**) *sdk2a*, and (**L**) *sdk2b* at 96 (arrows, compare L, I to C–F). All images displayed are of sections processed with antisense probe. Abbreviations: hpf=hours post fertilization; Sdk=sidekick; ONL=outer nuclear layer; INL=inner nuclear layer; GCL=ganglion cell layer; CMZ=ciliary marginal zone. Scale bar in A=50 µm (applies to all).

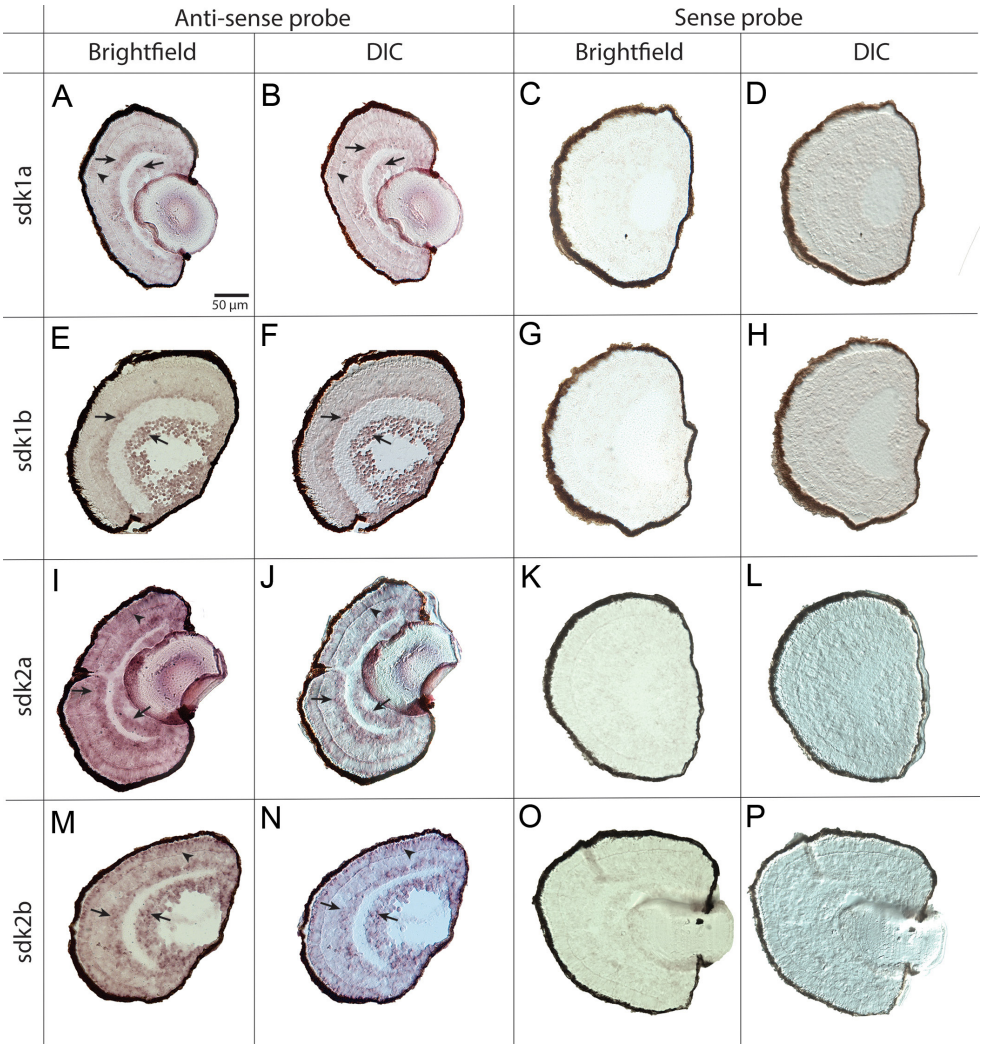

Figure 7. Bright-field and DIC imaging of antisense and sense in situ hybridization for *sdk* genes in cryosections. In situ hybridization using cryosections derived from 96 hpf zebrafish retina is shown for **A-D**) *sdk1a*, **E-H**) *sdk1b*, **I-L**) *sdk2a*, and **M-P**) *sdk2b*. **A,B,E,F,I,J,M,N**) In situ hybridization performed with antisense probes is shown. Arrows point to labeling in the inner nuclear layer (INL) and the ganglion cell layer (GCL); arrows point to labeling in the outer nuclear layer (ONL); asterisks show labeling in the ciliary marginal zone (CMZ). **C,D,G,H,K,L,O,P**) In situ hybridization performed with sense probes is shown. **A,C,E,G,I,K,M,O**) Photographs of antisense and sense in situ hybridization taken under bright-field conditions are shown. **B,D,F,H,J,L,N,P**) Photographs of antisense and sense in situ hybridization taken using DIC microscopy are shown. Abbreviations: DIC=differential interference contrast; hpf=hours post fertilization; Dscam=Down syndrome cell adhesion molecule; Sdk=sidekick. Scale bar in A=50 µm (applies to all).

zone (CMZ) of far peripheral retina (Figure 6C, F, I, L). The CMZ contains stem and progenitor cells that generate new retinal neurons and glia as the retina grows [44]. The extent of the expression domains of *sdk1a* and *sdk1b* appear to decrease over developmental time, while those of *sdk2a* and *sdk2b* appear to increase (Figure 6).

To ensure that the expression patterns observed were not a product of artifacts produced by the microscopy method used, cryosections were also imaged under bright-field and DIC for direct comparison (Figure 7A,B,E,F,I,JM,N). In addition, in situ hybridization controls using sense probes were performed for each *sdk* gene (Figure 7C,D,G,H,K,L,O,P).

Co-expression patterns of CAM gene paralogs during zebrafish retinogenesis: To determine whether our target CAM paralogs are co-expressed in the same cell populations, we used dual in situ hybridization in retinal sections obtained from 96 hpf zebrafish larvae. In these sections, co-expression of *dscama* and *dscamb* was observed within a subset of cells located in the GCL and INL (Figure 8A–C). However, only *dscamb* was strongly expressed in the ONL (Figure 8B). We also used dual in situ hybridization for the *sdk1* gene paralogs to determine if they are co-expressed during development. We found *sdk1a* and *sdk1b* were co-expressed by a subset of cells in the GCL and the basal portion of the INL (Figure 8D–F). Similarly, *sdk2a* and *sdk2b* were also found to be co-expressed by a subset of cells in the GCL, the basal portion of the INL, and the ONL (Figure 8 G–I).

Expression of dscam genes does not exclude expression of sdk1 or sdk2 genes: Dscam and *Sdk* genes are expressed in a mutually exclusive pattern in the chick retinal GCL [35] but are co-expressed in at least some common sets of neurons in mice [34,45]. We next sought to determine whether the expression of different CAM types was mutually exclusive in zebrafish retina. We performed dual in situ hybridization

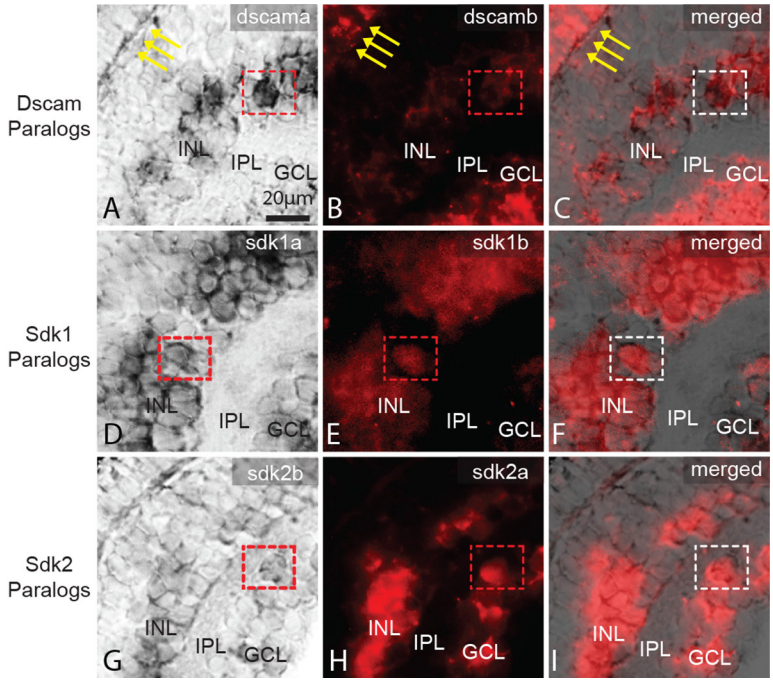

Figure 8. Expression of *dscam* and *sdk* paralogs in developing zebrafish central retina at 96 hpf. Comparative expression patterns of *dscama* versus *dscamb*, *sdk1a* versus *sdk1b*, and *sdk2a* versus *sdk2b* are shown following dual in situ hybridization. **A**: Expression of *dscama* was observed in the GCL and in the INL, but no expression was observed in the ONL (arrows). **B**: Expression of *dscamb* was observed in the GCL, INL, and ONL (arrows). **C**: Gene paralogs, *dscama*, and *dscamb* are co-expressed in some cells within the INL and GCL (boxed region), but only *dscamb* is expressed in the ONL (arrows). Yellow arrows point to the outer plexiform layer for viewer orientation. **D**: Expression of *sdk1a* was observed in the GCL and INL. **E**: Expression of *sdk1b* was seen in the GCL and INL. **F**: Gene paralogs *sdk1a* and *sdk1b* were co-expressed in some cells within the GCL and INL (boxed region). **G**: Expression of *sdk2b* was observed in the GCL and INL. **H**: Expression of *sdk2a* was observed in the GCL and INL. **I**: Gene paralogs *sdk2a* and *sdk2b* were co-expressed in some cells within the INL and GCL (boxed region). Dashed boxes show the identical region of interest (ROI) in each row. The red boxes correspond to the ROI for panels showing single-label expression in **A**, **B**, **D**, **E**, **G**, and **H**. White boxes in **C**, **F**, and **I** show ROIs of co-expression of paralogs. Abbreviations: hpf=hours post fertilization; Dscam=Down syndrome cell adhesion molecule; Sdk=sidekick; ONL=outer nuclear layer; INL=inner nuclear layer; GCL=ganglion cell layer. Scale bar in **A**=20 µm (applies to all).

in 96 hpf retinal sections with the following CAM gene pairs: *dscama* with *dscaml1, sdk1b* with *dscamb, sdk2b* with *dscamb,* and *sdk2b* with *sdk1b*. *Dscama* (Figure 9A) and *dscaml1* (Figure 9B) showed co-expression in a small number of cells located in the basal part of the INL (Figure 9C), while other areas of the INL only showed the expression of *dscaml1* or *dscama*. S*dk1b* (Figure 9D) and *dscamb* (Figure 9E) were co-expressed in some cells located in the INL and the GCL (Figure 9F). Similarly, *sdk2b* (Figure 9G) and *dscamb* (Figure 9H) were observed to have a similar pattern of sporadic co-expression within neurons of the INL and the GCL (Figure 9I); *sdk2b* (Figure 9J) and *sdk1b* (Figure 9 K), were observed to have occasional co-expression within the INL and the GCL (Figure 9L).

DISCUSSION

We report the predicted protein structures, gene structures, phylogenetic relationships, and developmental retinal expression patterns of the zebrafish genes encoding the Dscam and Sdk CAMs. The zebrafish has a richer repertoire of these CAM genes in their genomes, with duplicates (paralogs) of *dscam*, *sdk1*, and *sdk2* but not of *dscaml1*, while other vertebrate model organisms lack these duplicates. The paralogs likely did not arise through tandem duplication or retrotransposition because the duplicated genes are found in different chromosomes and because all the pairs of paralogs show the presence of introns (Figure 1B–E). Phylogenetic trees provide good support for the timing of duplication of the *dscam* genes (*dscama* and *dscamb*) and of the *sdk2* genes (*sdk2a* and *sdk2b*) as part of the TGD.

All the zebrafish CAM genes examined in this study are expressed within the developing retina, as summarized diagrammatically in Figure 10. The *dscams* are all expressed in the GCL and the INL, with occasional co-expression. *Dscamb* is also strongly expressed in the ONL, and *dscaml1* is also found in the outer INL, consistent with some degree of subfunctionalization of the paralogs (Figure 10A,B). *Sdk1a* and *sdk1b* show very similar expression domains in the INL, the GCL, and the CMZ. *Sdk2a* and *sdk2b* also show similar expression domains in the INL, the GCL, and the CMZ of all developmental stages examined, along with expression in the ONL of 96 hpf larvae (Figure 10C,D,E,F). However, in

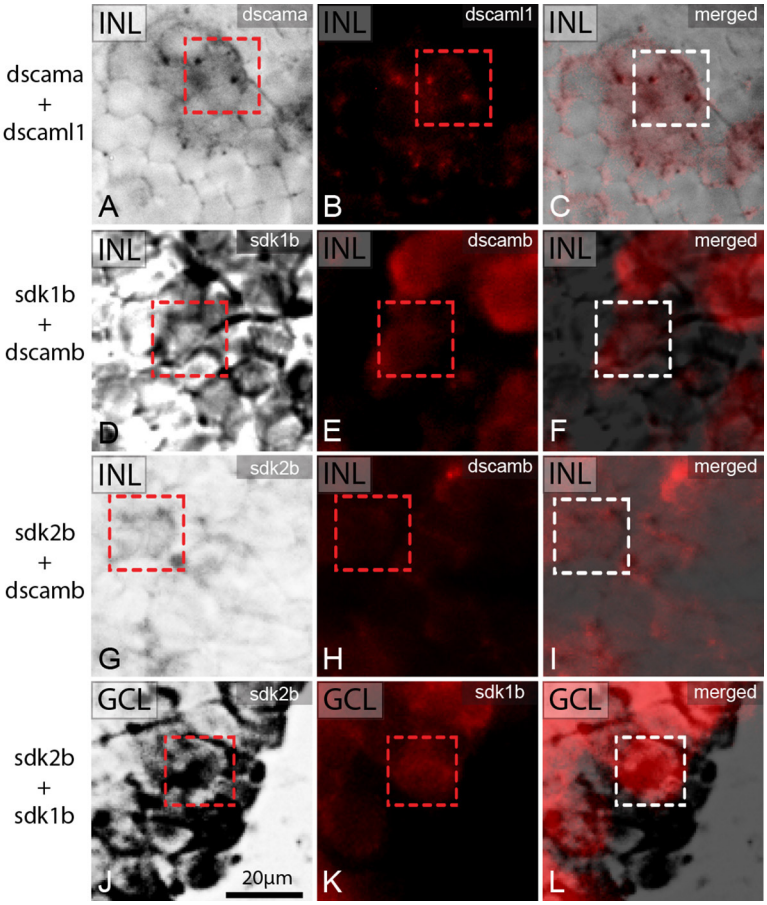

Figure 9. Comparative expression of *dscam* and *sdk* genes in the central inner retina of developing zebrafish at 96 hpf. Dual in situ hybridizations show comparative expression domains of CAM genes. **A**) *dscama* and **B**) *dscaml1*. **C**: Merged image reveals some co-expression within the INL (boxed region). **D**: *sdk1b* is expressed in a subset of cells within the basal INL. **E**: *dscamb* was also observed in the basal INL. **F**: The merged image shows some overlap in expression (boxed region). **G**: *sdk2b* expression was observed within the INL (boxed region). **H**: *dscamb* transcripts were also observed in the INL, and **I**: merging the two reveals low levels of co-expression (boxed region). **J**: *sdk2b* is expressed in a subset of cells within the INL. **K**: *sdk1b* expression is also observed in cells in the INL. **L**: The merged image reveals that some overlap exists between cells positive for both. For all comparisons, we observed a mosaic of cells expressing the two targeted transcripts—some cells that express both transcripts and other cells that express only one or the other. Dashed boxes show the identical region of interest (ROI) in each row. The red boxes correspond to the ROI for panels showing single-label expression in **A**, **B**, **D**, **E**, **G**, **H**, **J**, and **K**. White boxes in **C**, **F**, **I**, and **L** show ROIs of co-expression of paralogs. Abbreviations: hpf=hours post fertilization; Dscam=Down syndrome cell adhesion molecule; Sdk=sidekick; INL=inner nuclear layer; GCL=ganglion cell layer. Scale bar in **A**=20 µm (applies to all).

each case (*sdk1a* versus *sdk1b* and *sdk2a* versus *sdk2b*), these expression domains were not completely overlapping, again consistent with some degree of subfunctionalization (Figure 10C,D,E,F,G,H). We also note that the in situ probes used did not discriminate among predicted alternative splice products for *dscamb*, *dscaml1* (Figure 1C), *sdk1b* (Figure 1D), or *sdk2a* (Figure 1E); therefore, we may have undersampled the diversity of expression patterns of these CAMs. In addition, some of the CAM genes appeared to expand their expression domains, while others appeared to restrict these domains over developmental time. This finding is consistent with developmentally specific roles for the paralogs, for example, in cell–cell spacing within laminae versus later events, such as synaptogenesis.

Our results indicate that cellular expression patterns of *Dscam* and *Sdk* genes in the retina are not strictly conserved among vertebrates, with different vertebrate model species expressing different *Dscam* and *Sdk* genes in identified retinal cell types. *Dscama* is expressed in the GCL and the INL of the zebrafish retina (Figure 10A,B), which is consistent with the expression pattern of *Dscam* in the developing mouse retina [17] but differs from the expression pattern of Dscam in the chick retina, where subsets of cells in the ONL, all regions of the INL, and the GCL express *Dscam* [34]. Likewise, *Dscamb* is expressed in rods in the zebrafish ONL (43; Figure 10A,B), which differs from the mouse retina in which *Dscaml1*, but not *Dscam*, is expressed in rods [18]. Interestingly, *Dscam* is observed in the ONL of the developing chick retina, but in this case expression is enriched in green-sensitive cones [35,46].

The expression of zebrafish *sdk1* paralogs in the GCL and the INL (Figure 10C,D,E,F) is consistent with the expression of *Sdk1* in mouse retina, where there is expression in subsets of cells in the GCL and throughout the INL but very

little expression in the ONL [45]. The expression of *sdk2a* and *sdk2b* in 96 hpf zebrafish retina (Figure 10C,D,E,F) appears similar to the pattern of *Sdk* expression in the developing chick retina, in subsets of cells in the ONL, throughout the INL, and in the GCL [35,39].

Our results map the expression patterns of *dscam* and *sdk* genes in the zebrafish retina. According to the differential cell adhesion hypothesis, these combinatorial expression "codes" for retinal cell types may be important for the development of their spatial patterns and/or of their synaptic connections. Although the apparently distinct codes for zebrafish as compared to mice or chickens generate the same general retinal structure, the differences among species may underlie patterning features important for environmentally adaptive retinal functions, such as those related to color vision or high-acuity specializations. Why multiple proteins that mediate homotypic binding are co-expressed in individual cells is an open question. In mice co-expression of *Dscaml1* and *Sdk* genes in vglut3+ amacrine cells serve different roles, with *Dscaml1* preventing excessive adhesion and *Sdk* genes mediating synaptic lamination and pairing [34,45]. Compartment-specific roles for different CAMs may also explain the co-expression of multiple homotypic CAMs; for example, Dscam prevents adhesion in mouse RGC dendrites but promotes axon growth in RGC axons [18,20]. Differential binding of ligands, such as slit to Dscam but not Sdk proteins, may also explain the co-expression of multiple seemingly similar proteins [47]. In the future, we will perform functional studies to determine how the expression and co-expression of these genes influence the organization and circuitry of retinal neurons.

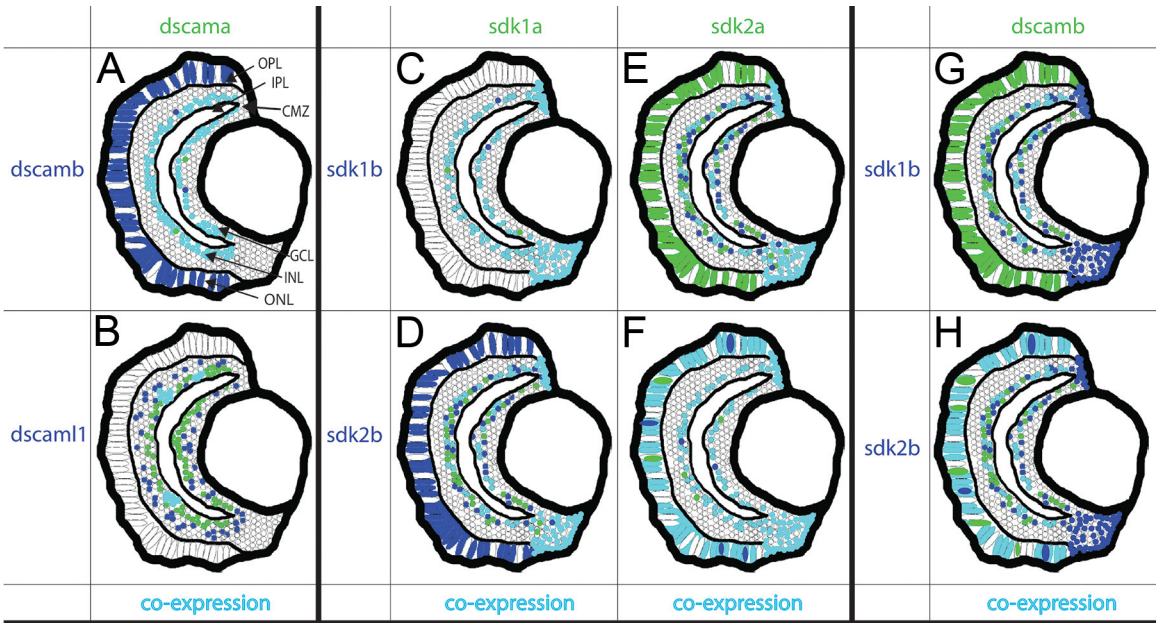

Figure 10. Diagrams of *dscam* and *sdk* expression patterns at 96 hpf. **A,B**: The *dscam* genes are all expressed in the GCL and inner INL, with occasional co-expression. **A)** shows the expression of *dscamb* and *dscama* where *dscamb* is also strongly expressed in the ONL. **B)** shows the expression of *dscaml1* and *dscama,* which are co-expressed in a subset of cells in the basal INL. *Dcamb* is also expressed in the ONL, and *dscaml1* is also found in the outer INL. **C-F)** The *sdk* genes were all expressed in the GCL, basal INL, and CMZ. **C)** *Sdk1a* and *sdk1b* show very similar expression domains in the INL, GCL, and CMZ. **D)** *Sdk1a* and *sdk2b* expression patterns were inferred from the almost complete co-expression of *Sdk1a* with *Sdk1b,* and the occasional co-expression of *sdk1b* and *sdk2b,* which indicates occasional co-expression in some cells in the GCL, INL, and CMZ of *sdk1a* and *sdk2b.* However, only *sdk2b* is present in the ONL. **E)** *Sdk2a* and *sdk1b* expression patterns were inferred from the almost complete co-expression of *sdk2a* with *sdk2b* and the occasional co-expression of *sdk2b* and *sdk1b,* which indicates occasional co-expression in some cells in the GCL, INL, and CMZ of *sdk2a* and *sdk1b.* However, only *sdk2a* is present in the ONL. **F)** *Sdk2a* and *sdk2b* also show similar expression domains in the INL, GCL, ONL, and CMZ of all developmental stages examined, along with expression in the ONL of 96 hpf larvae. **G,H)** The expression patterns of *dscam* and *sdk* genes are not mutually exclusive. **G)** *Dscamb* and *sdk1b* are sporadically co-expressed in some cells in the GCL and basal INL, while only *dscamb* is expressed in the ONL and only *sdk1b* is expressed in the CMZ. **H)** *Dscamb* and *sdk2b* are occasionally co-expressed in some cells in the GCL, basal INL, and ONL; however, only *sdk2b* is found in the CMZ. Abbreviations: hpf=hours post fertilization; Dscam=Down syndrome cell adhesion molecule; Sdk=sidekick; INL=inner nuclear layer; GCL=ganglion cell layer; ONL=outer nuclear layer, CMZ=ciliary marginal zone.

ACKNOWLEDGMENTS

This research was supported by NSF Cooperative Agreement DBI #093945 (BEACON; PGF), and NIH R21EY026814 (DLS). J. Sukeena was supported partially by a teaching assistantship from the University of Idaho. We thank Ruth Frey for assisting with in situ hybridization procedures training and Celeste Brown for assistance with phylogenetic analysis. Dr. Deborah L. Stenkamp (dstenkam@uidaho.edu) and Dr. Peter G Fuerst (fuerst@uidaho.edu) are co-corresponding authors for this study.

REFERENCES

1. Steinberg MS. Adhesion in development: an historical overview. Dev Biol 1996; 180:377-88. [PMID: 8954711].
2. Dean C, Dresbach T. Neuroligins and neurexins: linking cell adhesion, synapse formation and cognitive function. Trends Neurosci 2006; 29:21-9. [PMID: 16337696].
3. Galli-Resta L, Leone P, Bottari D, Ensini M, Rigosi E, Novelli E. The genesis of retinal architecture: An emerging role for mechanical interactions? Prog Retin Eye Res 2008; 27:260-83. [PMID: 18374618].
4. Sanes JR, Yamagata M. Many paths to synaptic specificity. Annu Rev Cell Dev Biol 2009; 25:161-95. [PMID: 19575668].
5. Matsuoka RL, Chivatakarn O, Badea TC, Samuels IS, Cahill H, Katayama K, Kumar SR, Suto F, Chédotal A, Peachey NS, Nathans J, Yoshida Y, Giger RJ, Kolodkin AL. Class 5 transmembrane semaphorins control selective Mammalian retinal lamination and function. Neuron 2011; 71:460-73. [PMID: 21835343].
6. Matsuoka RL, Nguyen-Ba-Charvet KT, Parray A, Badea TC, Chedotal A, Kolodkin AL. Transmembrane semaphorin signalling controls laminar stratification in the mammalian retina. Nature 2011; 470:259-63. [PMID: 21270798].
7. Duan X, Krishnaswamy A, Eap V, De la Huerta I, Sanes JR, Type II. Cadherins Guide Assembly of a Direction-Selective Retinal Circuit. Cell 2014; 158:793-807. [PMID: 25126785].
8. Peng YR, Tran NM, Krishnaswamy A, Kostadinov D, Martersteck EM, Sanes JR. Satb1 Regulates Contactin 5 to Pattern Dendrites of a Mammalian Retinal Ganglion Cell. Neuron 2017; 95:869-83. [PMID: 28781169].
9. Nevin LM, Taylor MR, Baier H. Hardwiring of fine synaptic layers in the zebrafish visual pathway. Neural Dev 2008; 3:36-[PMID: 19087349].
10. Mumm JS, Godinho L, Morgan JL, Oakley DM, Schroeter EH, Wong RO. Laminar circuit formation in the vertebrate retina. Prog Brain Res 2005; 147:155-69. [PMID: 15581704].
11. Dunn FA, Della Santina L, Parker ED, Wong RO. Sensory experience shapes the development of the visual system's first synapse. Neuron 2013; 80:1159-66. [PMID: 24314727].
12. Masland RH. The fundamental plan of the retina. Nat Neurosci 2001; 4:877-86. [PMID: 11528418].
13. Jaillon O, Aury JM, Brunet F, Petit JL, Stange-Thomann N, Mauceli E, Bouneau L, Fischer C, Ozouf-Costaz C, Bernot A, Nicaud S, Jaffe D, Fisher S, Lutfalla G, Dossat C, Segurens B, Dasilva C, Salanoubat M, Levy M, Boudet N, Castellano S, Anthouard V, Jubin C, Castelli V, Katinka M, Vacherie B, Biémont C, Skalli Z, Cattolico L, Poulain J, De Berardinis V, Cruaud C, Duprat S, Brottier P, Coutanceau JP, Gouzy J, Parra G, Lardier G, Chapple C, McKernan KJ, McEwan P, Bosak S, Kellis M, Volff JN, Guigó R, Zody MC, Mesirov J, Lindblad-Toh K, Birren B, Nusbaum C, Kahn D, Robinson-Rechavi M, Laudet V, Schachter V, Quétier F, Saurin W, Scarpelli C, Wincker P, Lander ES, Weissenbach J, Roest Crollius H. Genome duplication in the teleost fish Tetraodon nigroviridis reveals the early vertebrate proto-karyotype. Nature 2004; 431:946-57. [PMID: 15496914].
14. Zhang JZ. Evolution by gene duplication: an update. Trends Ecol Evol 2003; 18:292-8. .
15. Talbot WS, Hopkins N. Zebrafish mutations and functional analysis of the vertebrate genome. Genes Dev 2000; 14:755-62. [PMID: 10766732].
16. Schmucker D, Clemens JC, Shu H, Worby CA, Xiao J, Muda M, Dixon JE, Zipursky SL. Drosophila Dscam is an axon guidance receptor exhibiting extraordinary molecular diversity. Cell 2000; 101:671-84. [PMID: 10892653].
17. Hattori D, Millard SS, Wojtowicz WM, Zipursky SL. Dscam-mediated cell recognition regulates neural circuit formation. Annu Rev Cell Dev Biol 2008; 24:597-620. [PMID: 18837673].
18. Fuerst PG, Bruce F, Tian M, Wei W, Elstrott J, Feller MB, Erskine L, Singer JH, Burgess RW. DSCAM and DSCAML1 function in self-avoidance in multiple cell types in the developing mouse retina. Neuron 2009; 64:484-97. [PMID: 19945391].
19. Tadros W, Xu S, Akin O, Yi CH, Shin GJ, Millard SS, Zipursky SL. Dscam Proteins Direct Dendritic Targeting through Adhesion. Neuron 2016; 89:480-93. [PMID: 26844831].
20. Bruce FM, Brown S, Smith JN, Fuerst PG, Erskine L. DSCAM promotes axon fasciculation and growth in the developing optic pathway. Proc Natl Acad Sci USA 2017; 114:1702-7. [PMID: 28137836].
21. Westerfield M. The Zebrafish Book; A guide for the laboratory use of zebrafish (Danio rerio). Eugene, OR: University of Oregon Press; 2007.
22. Letunic I, Copley RR, Pils B, Pinkert S, Schultz J, Bork P. SMART 5: domains in the context of genomes and networks. Nucleic Acids Res 2006; 34:D257-60. [PMID: 16381859].
23. de Castro E, Sigrist CJ, Gattiker A, Bulliard V, Langendijk-Genevaux PS, Gasteiger E. Amos Bairoch, and Nicolas Hulo. ScanProsite: detection of PROSITE signature matches and ProRule-associated functional and structural residues in proteins. Nucleic Acids Res 2006; 34:W362-5-[PMID: 16845026].
24. Larkin MA, Blackshields G, Brown NP, Chenna R, McGettigan PA, McWilliam H, Valentin F, Wallace IM, Wilm A, Lopez R, Thompson JD, Gibson TJ, Higgins DG. Clustal W

and Clustal X version 2.0. Bioinformatics 2007; 23:2947-8. [PMID: 17846036].

25. Stamatakis A. RAxML-VI-HPC: maximum likelihood-based phylogenetic analyses with thousands of taxa and mixed models. Bioinformatics 2006; 22:2688-90. [PMID: 16928733].

26. Barthel LK, Raymond PA. Improved method for obtaining 3-microns cryosections for immunocytochemistry. J Histochem Cytochem 1990; 38:1383-8. [PMID: 2201738].

27. Nelson SM, Park L, Stenkamp DL. Retinal homeobox 1 is required for retinal neurogenesis and photoreceptor differentiation in embryonic zebrafish. Dev Biol 2009; 328:24-39. [PMID: 19210961].

28. Stevens CB, Cameron DA, Stenkamp DL. Plasticity of photoreceptor-generating retinal progenitors revealed by prolonged retinoic acid exposure. BMC Dev Biol 2011; 11:51-[PMID: 21878117].

29. Moraru C, Moraru G, Fuchs BM, Amann R. Concepts and software for a rational design of polynucleotide probes. Environ Microbiol Rep 2011; 3:69-78. [PMID: 23761233].

30. Mitchell DM, Stevens CB, Frey RA, Hunter SS, Ashino R, Kawamura S, Stenkamp DL. Retinoic Acid Signaling Regulates Differential Expression of the Tandemly-Duplicated Long Wavelength-Sensitive Cone Opsin Genes in Zebrafish. PLoS Genet 2015; 11:e1005483-[PMID: 26296154].

31. Doyle DA, Lee A, Lewis J, Kim E, Sheng M, MacKinnon R. Crystal structures of a complexed and peptide-free membrane protein-binding domain: molecular basis of peptide recognition by PDZ. Cell 1996; 85:1067-76. [PMID: 8674113].

32. Takahashi K, Nakanishi H, Miyahara M, Mandai K, Satoh K, Satoh A, Nishioka H, Aoki J, Nomoto A, Mizoguchi A, Takai Y. Nectin/PRR: an immunoglobulin-like cell adhesion molecule recruited to cadherin-based adherens junctions through interaction with Afadin, a PDZ domain-containing protein. J Cell Biol 1999; 145:539-49. [PMID: 10225955].

33. Yamagata M, Sanes JR. Synaptic localization and function of Sidekick recognition molecules require MAGI scaffolding proteins. J Neurosci 2010; 30:3579-88. [PMID: 20219992].

34. Garrett AM, Tadenev AL, Hammond YT, Fuerst PG, Burgess RW. Replacing the PDZ-interacting C-termini of DSCAM and DSCAML1 with epitope tags causes different phenotypic severity in different cell populations. eLife 2016; •••:5-[PMID: 27637097].

35. Yamagata M, Sanes JR. Dscam and Sidekick proteins direct lamina-specific synaptic connections in vertebrate retina. Nature 2008; 451:465-9. [PMID: 18216854].

36. Zou M, Guo B, He S. The roles and evolutionary patterns of intronless genes in deuterostomes. Comp Funct Genomics 2011; 2011:680673-[PMID: 21860604].

37. Yamakawa K, Huot YK, Haendelt MA, Hubert R, Chen XN, Lyons GE, Korenberg DSCAM Jr. a novel member of the immunoglobulin superfamily maps in a Down syndrome region and is involved in the development of the nervous system. Hum Mol Genet 1998; 7:227-37. [PMID: 9426258].

38. Schramm RD, Li S, Harris BS, Rounds RP, Burgess RW, Ytreberg FM, Fuerst PG. A novel mouse Dscam mutation inhibits localization and shedding of DSCAM. PLoS One 2012; 7:e52652-[PMID: 23300735].

39. Yamagata M, Weiner JA, Sanes JR. Sidekicks: synaptic adhesion molecules that promote lamina-specific connectivity in the retina. Cell 2002; 110:649-60. [PMID: 12230981].

40. Braasch I, Gehrke AR, Smith JJ, Kawasaki K, Manousaki T, Pasquier J, Amores A, Desvignes T, Batzel P, Catchen J, Berlin AM, Campbell MS, Barrell D, Martin KJ, Mulley JF, Ravi V, Lee AP, Nakamura T, Chalopin D, Fan S, Wcisel D, Cañestro C, Sydes J, Beaudry FE, Sun Y, Hertel J, Beam MJ, Fasold M, Ishiyama M, Johnson J, Kehr S, Lara M, Letaw JH, Litman GW, Litman RT, Mikami M, Ota T, Saha NR, Williams L, Stadler PF, Wang H, Taylor JS, Fontenot Q, Ferrara A, Searle SM, Aken B, Yandell M, Schneider I, Yoder JA, Volff JN, Meyer A, Amemiya CT, Venkatesh B, Holland PW, Guiguen Y, Bobe J, Shubin NH, Di Palma F, Alföldi J, Lindblad-Toh K, Postlethwait JH. The spotted gar genome illuminates vertebrate evolution and facilitates human-teleost comparisons. Nat Genet 2016; 48:427-37. [PMID: 26950095].

41. Postlethwait JH, Woods IG, Ngo-Hazelett P, Yan YL, Kelly PD, Chu F, Huang H, Hill-Force A, Talbot WS. Zebrafish comparative genomics and the origins of vertebrate chromosomes. Genome Res 2000; 10:1890-902. [PMID: 11116085].

42. Stenkamp DL. Development of the Vertebrate Eye and Retina. Prog Mol Biol Transl Sci 2015; 134:397-414. [PMID: 26310167].

43. Sun C, Galicia C, Stenkamp DL. Transcripts within rod photoreceptors of the Zebrafish retina. BMC Genomics 2018; 19:127-[PMID: 29422031].

44. Stenkamp DL. Neurogenesis in the fish retina. Int Rev Cytol 2007; 259:173-224. [PMID: 17425942].

45. Krishnaswamy A, Yamagata M, Duan X, Hong YK, Sanes JR. Sidekick 2 directs formation of a retinal circuit that detects differential motion. Nature 2015; 524:466-70. [PMID: 26287463].

46. Enright JM, Lawrence KA, Hadzic T, Corbo JC. Transcriptome profiling of developing photoreceptor subtypes reveals candidate genes involved in avian photoreceptor diversification. J Comp Neurol 2015; 523:649-68. [PMID: 25349106].

47. Alavi M, Song M, King GL, Gillis T, Propst R, Lamanuzzi M, Bousum A, Miller A, Allen R, Kidd T. Dscam1 Forms a Complex with Robo1 and the N-Terminal Fragment of Slit to Promote the Growth of Longitudinal Axons. PLoS Biol 2016; 14:e1002560-[PMID: 27654876].

Articles are provided courtesy of Emory University and the Zhongshan Ophthalmic Center, Sun Yat-sen University, P.R. China. The print version of this article was created on 19 July 2018. This reflects all typographical corrections and errata to the article through that date. Details of any changes may be found in the online version of the article.